Pergamon

Int. J. Heat Mass Transfer. Vol. 37, No. 15, pp. 2203–2210, 1994

0017–9310/94 $7.00+0.00

0017–9310(94)E0057–2

Experimental study on mass transfer from a circular cylinder in pulsating flow

HYUNG JIN SUNG, KWON SANG HWANG and JAE MIN HYUN

Department of Mechanical Engineering, Korea Advanced Institute of Science and Technology, 373-1 Kusong-dong, Yusong-ku, Taejon 305-701, South Korea

(*Received* 30 *September* 1993 *and in final form* 24 *February* 1994)

Abstract—Laboratory measurements were made of local mass transfer from a cylinder, which is placed in a pulsating free stream, $U = U_0(1 + A_0 \cos 2\pi f_p t)$. Low turbulence-intensity wind tunnel experiments were conducted for small and moderate Reynolds numbers, $4500 \leqslant Re_d \leqslant 12450$. Pulsation was generated by means of an acoustic speaker. Mass transfer rates were measured by employing the naphthalene sublimation technique. The present results for non-pulsating flows ($A_0 = 0.0$) were shown to be consistent with the published data. For pulsating approach flows, plots were constructed to illustrate the distribution of the Sherwood number, Sh, as a function of the azimuthal angle θ measured from the front stagnation point. In the zone of attached boundary layer, the effect of pulsation on Sh is meager. Sh decreases monotonically from the maximum value at the front stagnation point to the minimum value near the separation point $\theta \approx 80$–$90°$. In general, Sh increases appreciably with increasing θ, after passing the separation point. The curve of Sh contains a secondary minimum point at around $\theta \approx 130$–$150°$. The general magnitude of Sh increases, as A_0 increases. The augmentation of mass transfer is more pronounced for large f_p such that the flow lock-on phenomenon takes place. At large Re_d, the relative influence of pulsation on Sh weakens.

1. INTRODUCTION

FLOW CHARACTERISTICS around a circular cylinder, which is placed normal to the approach stream, constitute a classical problem. The flow separation from the body and the wake structure are important topics from the standpoint of fundamental research as well as in technological applications. If the Reynolds number of the free stream is large, the unsteady shedding in the wake poses a prominent subject. There is a large body of technical literature [1–3] revealing the salient flow characteristics when the approach free stream is steady and uniform at U_0.

Recently, considerable attention has been given to the case when the free stream is time-dependent. In actual applications, the unsteadiness of the free stream may stem from the externally-generated turbulence or organized pulsations. For precise dynamic modeling, studies have delineated the essential features of flow around the cylinder when the free stream contains a well-defined single-frequency pulsation. These investigations looked into the vortex shedding patterns, especially when the pulsation frequency f_p of the approach stream is close to or above the natural shedding frequency f_{s0} of the system. Among others, the lock-on phenomenon, in which the vortex-shedding frequency f_s is intimately linked to f_p, occupied the center stage. Many issues pertinent to the interactions of flow with a fixed cylinder have been dealt with by prior investigations [4–6].

In contrast to the proliferation of interest on the flow characteristics, published accounts on heat and/or mass transfer properties from the cylinder to the pulsating approach stream are relatively scarce, and the results tend to be incomplete [7–9]. In a related work, Andraka and Diller [8] experimentally examined the effects of sinusoidal flow pulsation on heat transfer from a cylinder placed in a turbulent pulsating free stream, which was assumed to be expressible as $U = U_0(1 + A_0 \cos 2\pi f_p t)$. The pulsation amplitudes A_0 of up to 25% and pulsation frequencies f_p both above and below the natural shedding frequency f_{s0} were encompassed. These experiments registered no significant increase of time-averaged local heat transfer from the cylinder due to the pulsation. Gundappa and Diller [9] performed experiments by carefully distinguishing the effects between three-dimensional turbulence and one-dimensional organized sinusoidal pulsation. The results also indicated no measurable impact of the pulsation on heat transfer. It should be mentioned that, in these studies, the range of the Reynolds number was relatively high, $Re_d = 35000$–164000, although the majority of data presented were for a single value of $Re_d = 50000$. Clearly, more systematic parametric studies would be helpful to disclose the details of local behavior of transfer properties from the cylinder surface.

The aim of the present paper is to explore the local mass transfer from the cylinder surface when the free

NOMENCLATURE

A_0	pulsating amplitude	Δt	naphthalene sublimation thickness
d	diameter of the cylinder	T	temperature
D_f	mass diffusion coefficient for naphthalene vapor in air	U	freestream velocity
		U_0	freestream mean velocity.
Eu	power spectrum of velocity fluctuations		
f_p	pulsating frequency	Greek symbols	
f_s	shedding frequency	ν	kinematic viscosity
f_{s0}	natural shedding frequency	θ	circumferential angle from the front stagnation point
h_m	local mass transfer coefficient		
m''	local naphthalene mass transfer rate per unit area of the cylinder surface	ρ_s	density of solid naphthalene
		$\rho_{v,w}$	density of naphthalene at the wall
P_v	vapor pressure of naphthalene	ρ_ω	vapor density of naphthalene in freestream
R	universal gas constant		
Re_d	Reynolds number ($Re_d = Ud/\nu$)	$\Delta\tau$	exposure time
Sh	Sherwood number	τ	measurement time.

stream contains a well-defined single-frequency pulsation. Emphasis is placed on documenting the local mass transfer characteristics over low and moderate Reynolds numbers, i.e. $4500 \leqslant Re_d \leqslant 13\,500$. In particular, the study is focused on the circumferential variation of the Sherwood number, Sh. The primary parameters of pulsation, namely, the pulsation amplitude A_0 and frequency f_p, are allowed to have wider variations than in the studies of Andraks and Diller [8] and Gundappa and Diller [9]. Of interest are the situations in which f_p increases beyond the natural shedding frequency f_{s0}. The transfer properties in the forward stagnation zone and in the separation region will be described in detail.

In the present experiments, measurements of mass transfer were obtained by employing the well-established naphthalene sublimation technique in a specially-designed wind tunnel. This method has been successfully utilized in various types of mass transfer research [10–12], and it proves to be a viable experimental tool for the present problem.

2. EXPERIMENTAL APPARATUS AND PROCEDURE

An open-circuit blower-type wind tunnel was used for the experiment. The air speed at the test section (250×250 mm) was varied from 1.5 to 22.0 m s^{-1}, and the turbulence intensity of free stream in the test section was less than 0.3%. The diameter of the cylinder, which was made of steel, was 25.0 mm. This gives a blockage factor of 0.1.

The pulsation of the free stream was achieved by placing a speaker in the settling chamber. The sinusoidal signal was produced by means of a function generator. This signal was passed through an audio amplifier, and it then was sent to the speaker. It is of interest that, in the experiment of Andraka and Diller [8], the flow pulsation was created mechanically, i.e. by mounting six rotating shutters on parallel shafts in the settling chamber. It is believed that the method of producing pulsation by acoustic means, as in the present work, leads to a simple and straightforward experimental design [4].

The mean velocity distributions in the test section were measured by using a standard Pitot tube. In order to monitor the turbulent intensity as well as the pulsation amplitude and frequency of free stream, an I-type hot wire was utilized.

Care was exercised in dealing with the naphthalene sublimation technique, which formed the heart of the present mass transfer experiments. Two pieces of copper mold, 80.0 mm long and 25.0 mm thick, were fabricated. The cylinder was inserted inside the mold. The molten naphthalene was poured into the bottom side of the two injection holes. The portion of the cylinder, which was naphthalene-cast, was finished to ensure that it had the same diameter as the steel part. In order to measure the sublimated naphthalene, an automated data acquisition system was installed. The main components were a depth gauge with a signal conditioner, a digital voltmeter connected to a GPIB interface, a positioning apparatus driven by stepper motors and an IBM-486 personal computer. The circumferential variation of the naphthalene sublimation thickness was determined by employing a depth gauge. Prior to each reading, the gauge was allowed a 0.5-s stabilization period. The measurement of the naphthalene surface profile was performed at constant room temperature, which would alleviate possible errors caused by natural convection.

The spanwise variations of flow and mass transfer properties were checked, and they were found to be very small, within 1.0%. Therefore, all the measurements were taken in the central symmetry plane of the cylinder, and the two-dimensionality was taken to be

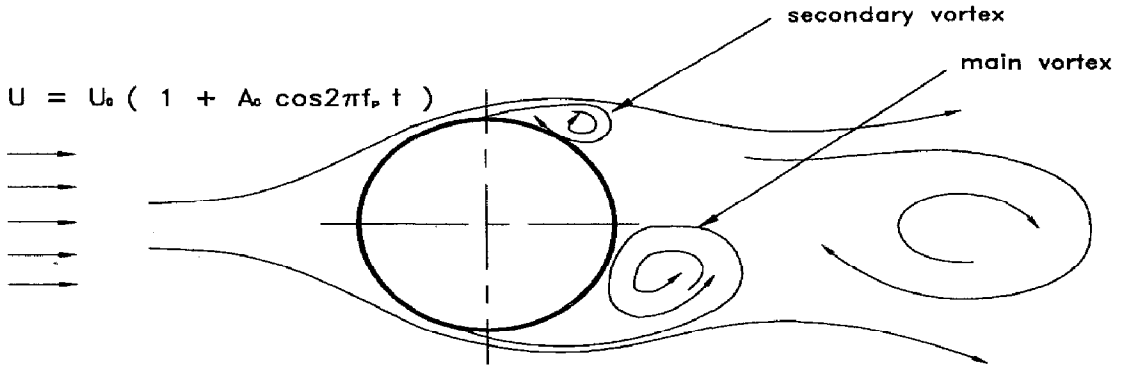

FIG. 1. Schematic view of the flow configuration.

an adequate approximation. A schema of the flow geometry is shown in Fig. 1.

The naphthalene sublimation technique has been refined for precise measurements of mass transfer, and the full implications of this method have been thoroughly documented [11, 12]. The mass transfer coefficient h_m can be derived as:

$$h_m = \rho_s(\Delta t/\Delta\tau)/\rho_{v,w} \quad (1)$$

in which ρ_s and $\rho_{v,w}$ denote, respectively, the density of naphthalene ($\rho_s = 0.975$ kg m^{-3} at 25°C) and the naphthalene vapor concentration at the wall. Here Δt represents the thickness of the naphthalene sublimation during the time period $\Delta\tau$. It then follows that the Sherwood number Sh is given as:

$$Sh = h_m d/D_f \quad (2)$$

in which d is the cylinder diameter and D_f the diffusivity of naphthalene. Explicit details, including the relationship between $\rho_{v,w}$ and the local temperature T, are available (e.g. Sung *et al.* [12]).

Experimental uncertainties in the present procedures can be estimated. Possible elemental sources of uncertainties are the determination of the material properties (approximately 4%) and the measurement errors. The bulk of the errors stems from the resolution limitation of the positioning of the apparatus. In accordance with the error predictions of Sung *et al.* [12], the uncertainties in the total sublimation depth are appraised to be approximately 5% for an exposure time of about 100 min. The combined error analysis concludes that the overall uncertainty in the evaluation of h_m is approximately 10%.

3. RESULTS AND DISCUSSION

The first task was to assess the quality of the pulsation superimposed on the uniform free stream. To this end, the power spectrum of the free stream velocity field data obtained by the I-type hot wire was analysed. Based on extensive surveys of the free stream velocity fields, the oncoming velocity has been found, to a reasonable degree of accuracy, to have a sinusoidal pulsation, i.e. expressible by $U = U_0(1 + A_0 \cos 2\pi f_p t)$. Figure 2 illustrates the exemplary velocity signals and their power spectra. These results indicate that the present acoustic method is a viable technique to produce high-quality pulsations in the free stream. The turbulence intensity in the oncoming stream was measured to be smaller than 0.3%. For the wind-tunnel test rig of the present study, the majority of experiments were carried out in the ranges of $f_p \approx 10.0$–40.0 Hz, $A_0 \approx 0.08$–0.23.

Preliminary analyses were conducted to examine the major features of the wake flow. Figures 3 and 4 are presented to demonstrate the lock-on phenomenon and the influence in relevant parameters. As displayed in Fig. 3a, if the approach flow is non-pulsating ($A_0 = 0.0$), the vortex shedding patterns in the wake are characterized by the natural shedding frequency, f_{s0} ($\approx$21.0 Hz). Since vortex shedding is

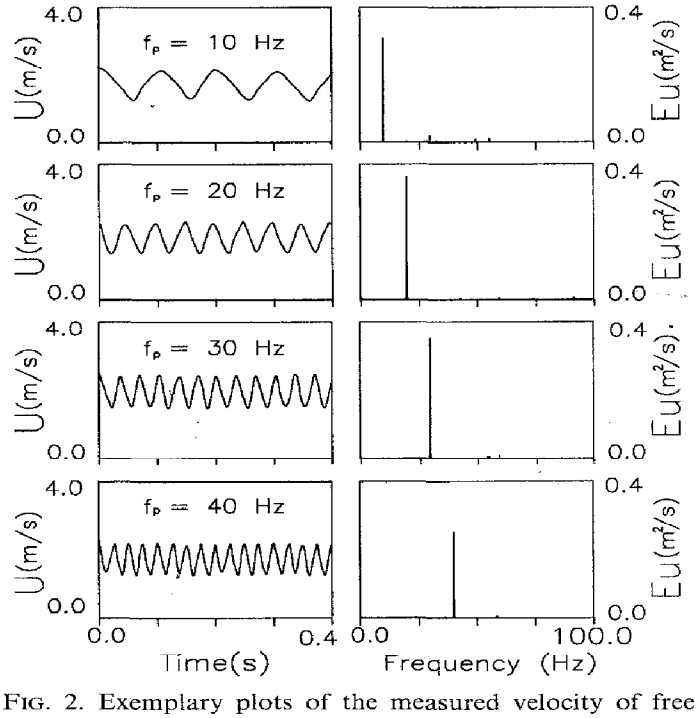

FIG. 2. Exemplary plots of the measured velocity of free stream, U, and its power spectrum, Eu.

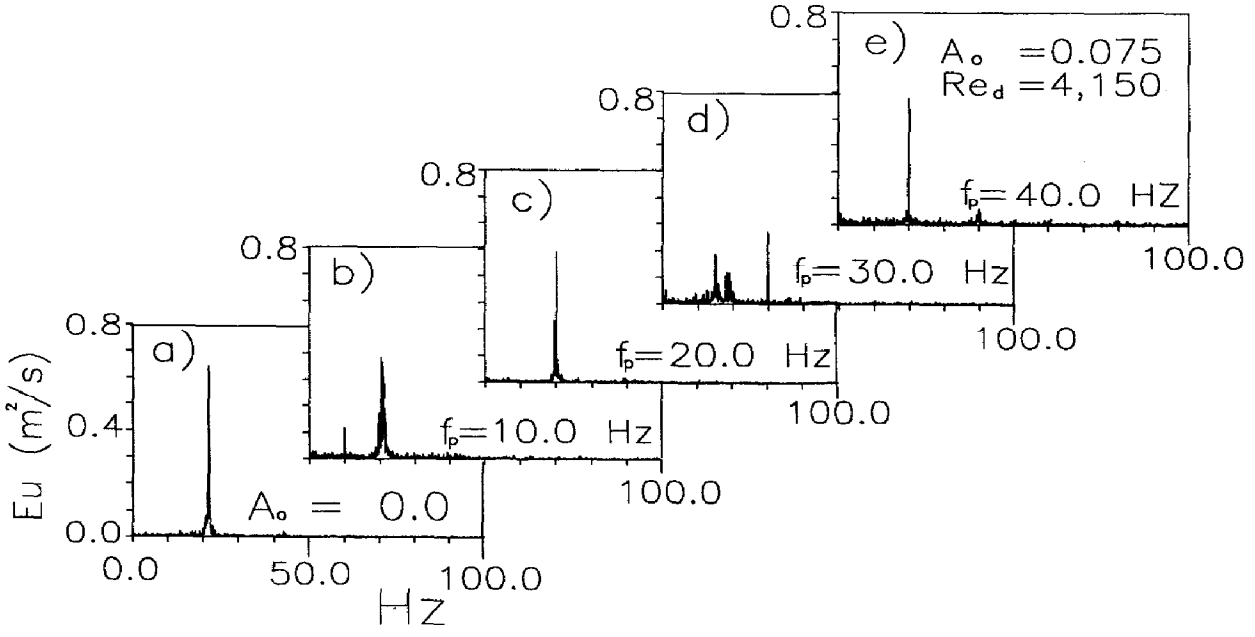

FIG. 3. Power spectra of the measured velocity in the wake: (a) $A_0 = 0.0$, conditions for (b), (c), (d), (e) are $A_0 = 0.075$, $Re_d = 4150$ and $f_{s0} = 21.0$ Hz.

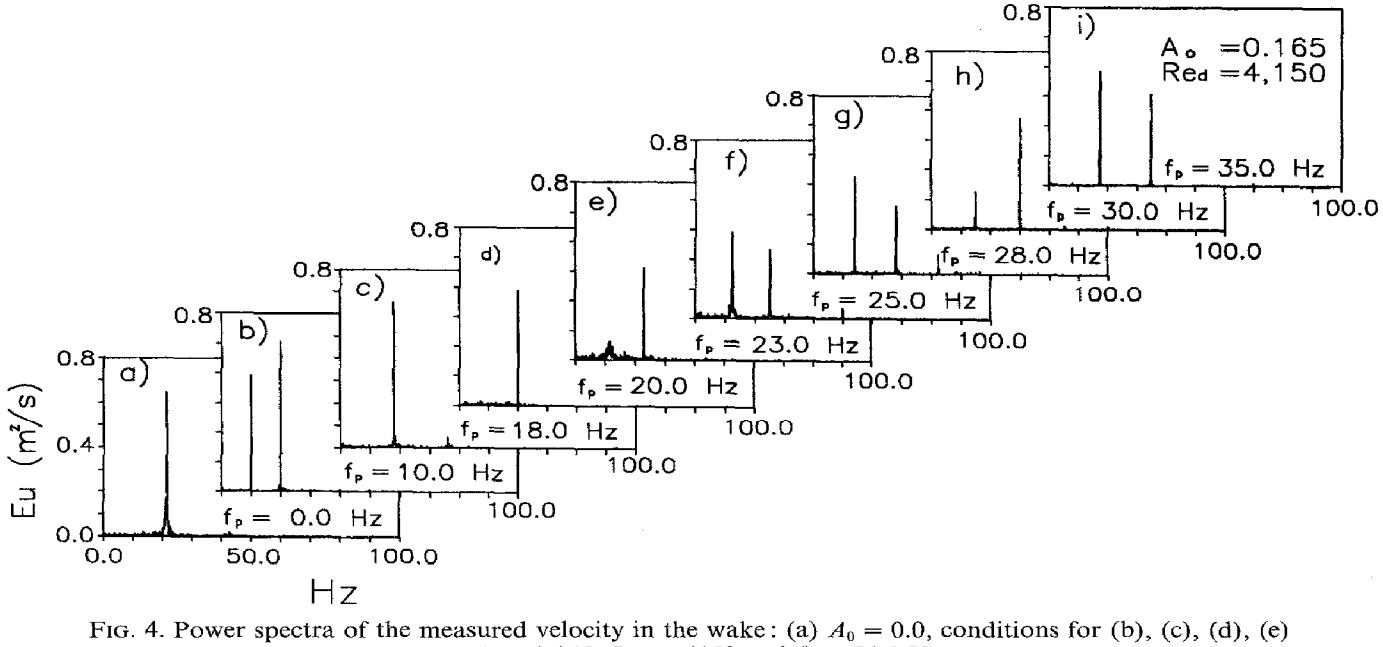

FIG. 4. Power spectra of the measured velocity in the wake: (a) $A_0 = 0.0$, conditions for (b), (c), (d), (e) are $A_0 = 0.165$, $Re_d = 4150$ and $f_{s0} = 21.0$ Hz.

caused primarily by alternating rolling-up of the separated shear layer, the influence of pulsation is appreciable. When f_p is much smaller than f_{s0}, the dominant frequency of vortex shedding is still at f_{s0}, but a subharmonic frequency is also discernible for the wake flows (see Fig. 3b). However, when f_p exceeds f_{s0}, the shedding patterns show additional complexities. As illustrated in Fig. 3d, the power spectrum of the wake flows contains two peak frequencies, one at f_p and the other near $0.5 f_p$. If f_p is much greater than f_{s0}, the celebrated lock-on phenomenon is evident in Fig. 3e. Much of the vortex shedding in the wake is characterized by a single frequency f_s, which is 0.5 f_p. This salient feature of lock-on, i.e. the shedding frequency is locked-on to $0.5 f_p$, has been disclosed in a number of unsteady fluid dynamics research [5, 6]. The observations of Fig. 3 are supportive of these well-established contentions of lock-on, and the results also lend credence to the viability of the present experiments. Similar trends are also visible in Fig. 4, but with a slightly increased value of A_0 ($A_0 = 0.165$). It is noticeable in Fig. 4 that the peaks in the power spectrum are more distinct than in Fig. 3. In other words, as A_0 increases, the relative magnitudes of the

general noise levels of the spectrum are reduced. The above findings serve to reconfirm the much-discussed features of unsteady flow past a cylinder [5–7].

The mass (and/or heat) transfer properties from a circular cylinder to a non-pulsating uniform crossflow ($A_0 = 0.0$) have long been investigated by many authors [10, 11, 13–16]. In the case of laminar flow, the flow separation is known to take place somewhere less than $\theta = 90°$ measured from the front stagnation point. The Sherwood number Sh takes a maximum value in the front stagnation zone, and Sh gradually decreases along the downstream circumferential direction, as the boundary-layer thickens along the way. As the flow reaches the separation region, the thickness of the boundary-layer becomes appreciable, and the mass transfer is reduced accordingly. After passing the separation region, Sh increases slightly as the flow tends to the rear stagnating point. These are attributed to the generation of secondary flow, which is accompanied by augmented mixing by recirculating flows.

In the actual experiments, the mass transfer data were acquired at a 0.72° interval in the circumferential direction. This circumferential resolution is comparable to or higher than the previous laboratory data of mass transfer experiments for a non-pulsating flow [10, 16].

Figure 5 exhibits the diagrams of Sh vs the circumferential angle θ for non-pulsating flows ($A_0 = 0.0$). These are designed to validate the present measurements by checking them against the existing

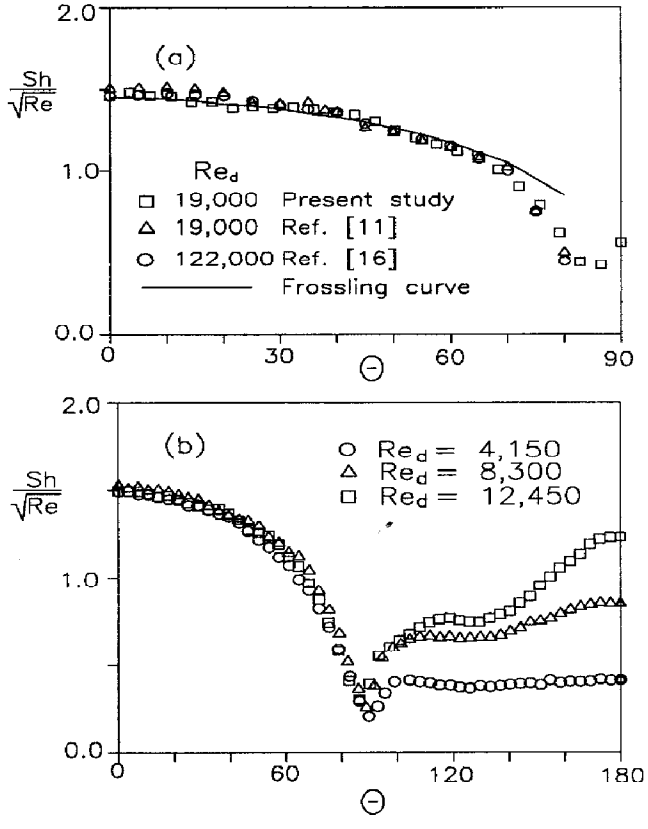

FIG. 5. Local mass transfer measurements for a non-pulsating flow ($A_0 = 0.0$).

data. In accordance with the theoretical prediction by Frossling and other laboratory observations [11, 16], the ordinate is shown in $Sh/Re_d^{1/2}$. Figure 5a illustrates the behavior in the forward portions of the cylinder. Near the separation region around $\theta = 90°$, mass transfer reaches a minimum. As is conspicuous in Fig. 5a, the present experiments are consistent with the existing laboratory data. Also shown in the figure is the theoretical prediction of Frossling (shown in solid line), which is derived for the region of attached boundary-layer before arriving at the separation zone. Minor discrepancies between the measurement sets are attributable to the differences in turbulent intensity and in the tunnel blockage effects and other experimental conditions [10]. Figure 5b exhibits that mass transfer increases in the rear portions of the cylinder after passing the separation zone. The intensification of mass transfer in this region ($90° \leqslant \theta \leqslant 180°$), with the increase of Re_d, is clearly captured in Fig. 5b. These trends are consistent with the results of heat transfer measurements of Andraka and Diller [8].

Now, the mass transfer properties for a pulsating crossflow are scrutinized in Figs. 6–8. Firstly, the impact of f_p is exemplified in Fig. 6. For this set of parameter values, the natural shedding frequency is found to be approximately $f_{s0} = 21.0$ Hz. The effect of pulsation on the mass transfer rate is seen to be very small in the region of attached boundary-layer, say, $0.0 \leqslant \theta \leqslant 90°$. In related studies on heat transfer characteristics [8, 17], the influence of pulsation on heat transfer in this region was also found to be meager, which is in qualitative accord with the present observations. One plausible argument is that, in the region of attached laminar boundary layer, the lowest-order time-averaged net effect of pulsation tends to be very small. However, a drastically different picture emerges on the region downstream of the separation zone. As is apparent in the plots, mass transfer is augmented in this region by pulsation. The mass transfer enhancement is more pronounced, as f_p increases, especially when f_p is beyond f_{s0}. Also, as easily anticipated, mass transfer augmentation by pulsation is more vigorous as A_0 increases.

A closer inspection of Fig. 6 discloses that the Sh-curves may be divided into three qualitatively distinct regions: (i) the region of attached boundary layer, which extends from the front stagnation point to the separation zone (minimum point of Sh); (ii) the region between the separation zone and the zone of a milder secondary minimum of the Sh-curves, typically around $\theta_1 = 140.0°$; (iii) the region that extends from θ_1 to the rear stagnation point, $\theta_1 \leqslant \theta \leqslant 180°$. The above classification was originally introduced by Boulos and Pei [18] for turbulent heat transport from a cylinder. However, a qualitatively similar description is applicable to the present mass transfer measurements. As expounded by Boulos and Pei, region (ii) corresponds to the cylinder surface area whereby the small secondary vortices are active (see Fig. 1). These small vortices are entrained by the free shear layer,

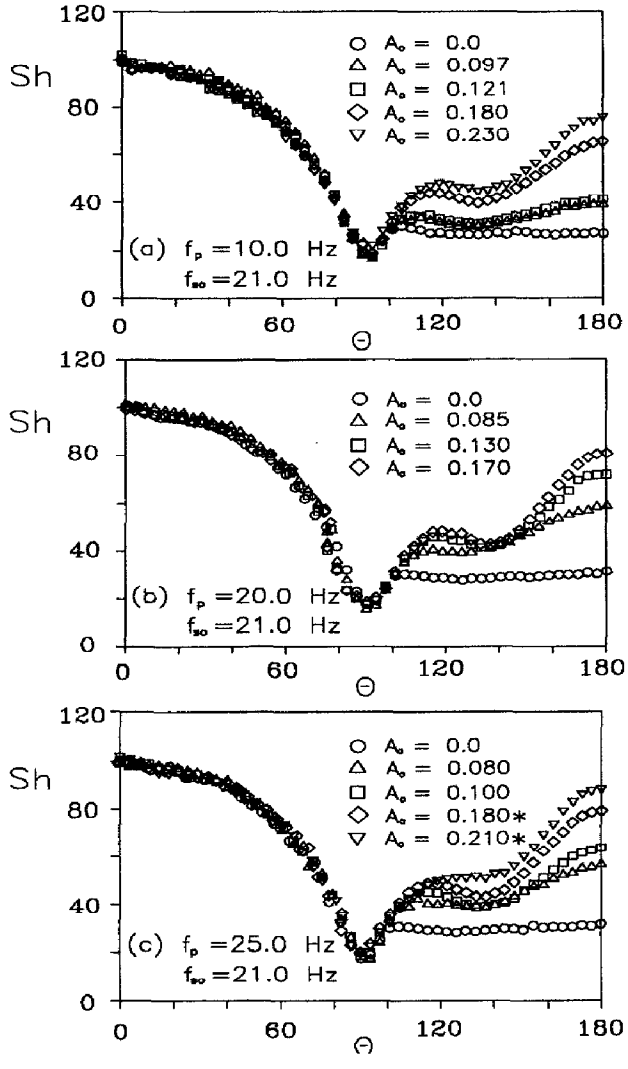

FIG. 6. Local mass transfer measurements for pulsating flows: (a) $f_p = 10.0$ Hz; (b) $f_p = 20.0$ Hz; (c) $f_p = 25$ Hz, $Re_d = 4150$ and $f_{so} = 21.0$ Hz (* indicates lock-on).

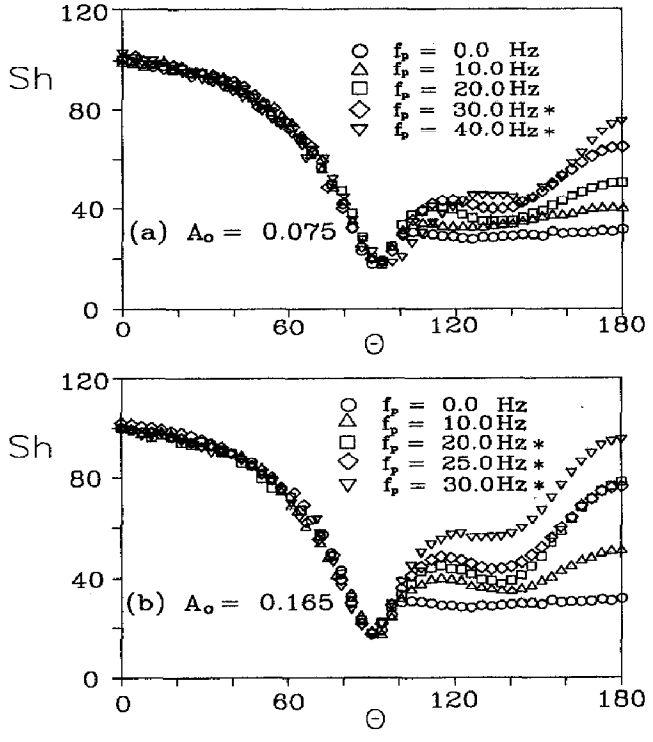

FIG. 7. Local mass transfer measurements for pulsating flows: (a) $A_0 = 0.075$; (b) $A_0 = 0.165$, $Re_d = 4150$ and $f_{s0} = 21.0$ Hz (* indicates lock-on).

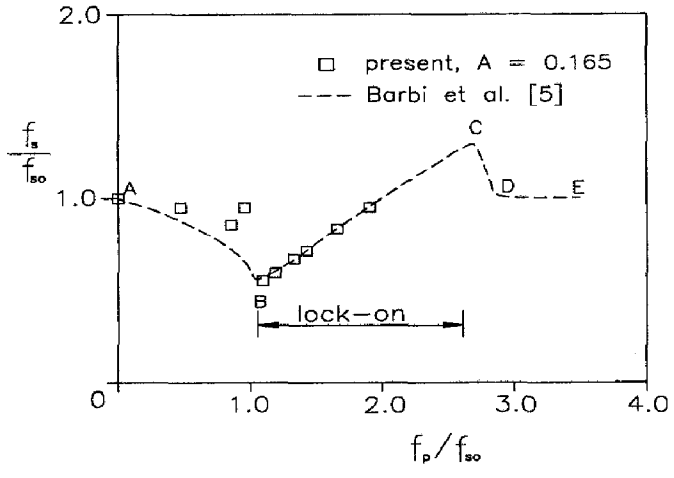

FIG. 8. Illustrative plot showing the general relation between the shedding frequency f_s and the pulsating frequency f_p; $A_0 = 0.165$, $f_{s0} = 21.0$ Hz.

and they coalesce with the main vortex behind the cylinder. The demarcation lines of region (ii) oscillate over the cylinder surface, in tune with the shedding frequency f_s. Region (iii) represents the cylinder surface which subtends the main vortex, as sketched in Fig. 1. This overall qualitative depiction of the principal flow features is useful for physical characterizations of the present mass transfer data.

It is evident in Fig. 6 that the invigoration of mass transfer is more effective in region (iii) than in region (ii). This suggests that pulsation causes faster mixings of vortices in the rear end of cylinder. Furthermore, this phenomenon is more prominent at high values of f_p at which lock-on takes place.

Replotting the data for easier inspection, the effect of A_0 is explicitly shown in Fig. 7. These measurements clearly demonstrate that the pulsation of the free flow gives rise to an increase in Sh in the region downstream of the separation zone. Comparison of Fig. 7a and b suggests that, as A_0 increases, the position of the secondary minimum point of Sh moves to a slightly further downstream location. Boulos and Pei [18] stated that the demarcation between region (ii) and region (iii) oscillates at the shedding frequency f_s around $\theta = 130$–$150°$. When A_0 is large (see Fig. 7b), the enhancement of mass transfer is seen to be substantial in region (iii), and this is pronounced for lock-on pulsating frequencies ($f_p \geqslant 20.0$ Hz).

The general relationship between the shedding frequency f_s, and the pulsation frequency f_p, is well documented. This is illustrated in Fig. 8, which is based on the results of Barbi *et al.* [5]. In the section A–B of Fig. 8, when f_p is reasonably small, not much variation

of f_s is seen from the value f_{s0}, which corresponds to the shedding frequency for a non-pulsating oncoming flow. In the intermediate range of f_p, shown in B–C in Fig. 8, lock-on occurs. This is characterized by a well-established relation, $f_s = 0.5f_p$. In this range, as f_p increases, the shedding frequency increases in proportion to f_p. As emphasized by Barbi *et al.* [5], when lock-on takes place, vortices in the rear portions of the cylinder tend to get more attached to the cylinder surface as they form and grow. The fundamental flow structure was explained in detail by Barbi *et al.* This phenomenon becomes more intensified at higher values f_p in the range of lock-on. This is reflected in enhanced mass transfer, which leads to higher values of *Sh*. However, when f_p increases beyond the range of the lock-on regime (C–D–E in Fig. 8), the behavior of f_s shows a smooth transition toward the value f_{s0} [5]. In this range of very large f_p (D–E in Fig. 8), f_s returns to the natural shedding frequency. Consequently, *Sh* is thought to decrease from its maximum value exhibited at the value of f_p corresponding to point C in Fig. 8. In the present experiment, the upper limit of the pulsation frequency was imposed by practical laboratory constraints. Therefore, no experimental data of *Sh* were produced in the present experiment when f_p is larger than the upper limit of the lock-on range.

Figure 9 exhibits the effect of the Reynolds number. It is noted that the relative impact of the pulsation decreases as Re_d increases. As revealed in Fig. 9c, at large Re_d, the *Sh*-curves remain substantially unchanged by the addition of pulsation. This could be attributed to the fact that the vortex shedding in the wake is little influenced by the pulsating components, if the overall Reynolds number of the oncoming flow is very large. Alternatively speaking, when Re_d is large, the natural shedding frequency f_{s0} is much larger than the values of f_p used in the experiments. This implies that there would be few interactions between the pulsation components and the vortices in the wake.

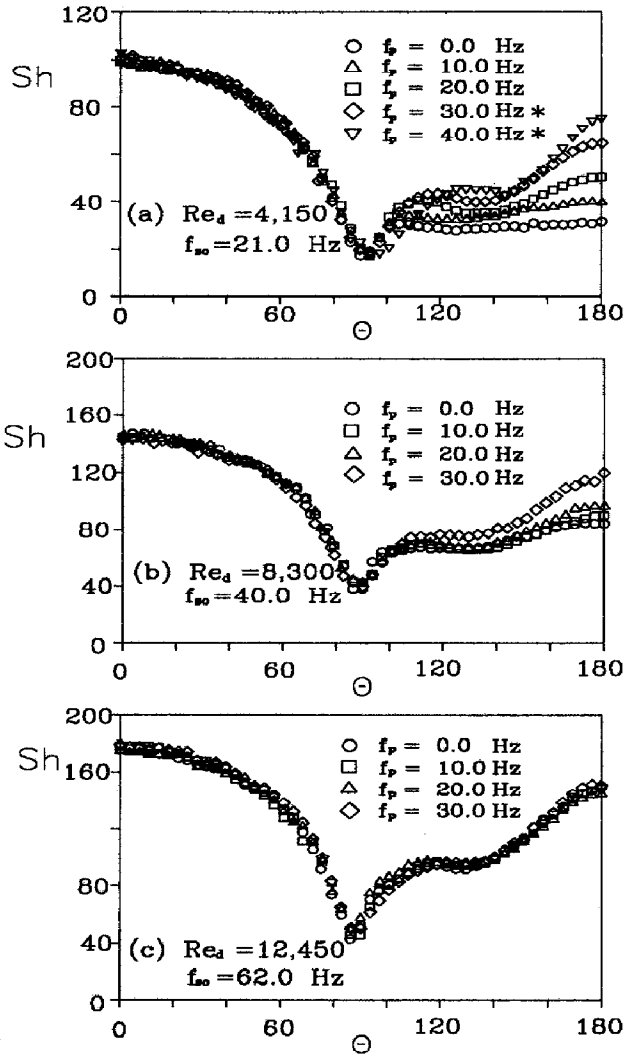

FIG. 9. Local mass transfer measurements for pulsating flows of $A_0 = 0.075$: (a) $Re_d = 4150$ and $f_{s0} = 21.0$ Hz; (b) $Re_d = 8300$ and $f_{s0} = 40.0$ Hz; (c) $Re_d = 12\,450$ and $f_{s0} = 62.0$ Hz (* indicates lock-on).

4. CONCLUSION

Detailed measurements of local mass transfer from a cylinder were obtained by exploiting the naphthalene sublimation technique. The oncoming free stream contains a well-defined single-frequency pulsation.

For non-pulsating free streams ($A_0 = 0.0$), the Frossling number, $Sh/Re^{1/2}$ decreases monotonically from the peak value at the front stagnation point to the minimum value in the separation zone. Further downstream past the separation zone, mass transfer increases appreciably, and this increase is more pronounced at high Re_d.

For a pulsating free stream, three qualitatively distinct regions are identified. The effect of pulsation is weak in region (i), which extends from the front stagnation point to the separation zone. In region (ii), in which the secondary vortices are active, *Sh* increases appreciably. Further increases in *Sh* are noted in region (iii) of the cylinder surface, which subtends the zone of main vortex. The *Sh*-curve has the primary minimum in the separation zone, approximately at $\theta \approx 90°$, and a mild secondary minimum at the border between region (ii) and region (iii), $\theta \approx 130$–$150°$.

The impact of the flow pulsation is seen to enhance mass transfer in the downstream locations after the separation. This enhancement of *Sh* is more effective as A_0 increases. Also, *Sh* is augmented as f_p increases; the increases in *Sh* are more pronounced for high f_p such that the flow lock-on phenomenon takes place. The relative influence of pulsation on *Sh* tends to decrease as Re_d becomes large. When Re_d is very high, the natural shedding frequency f_{s0} is much larger than f_p used in the experiment. Consequently, the effect of

pulsation on Sh is minor for such very high values of Re_d.

Acknowledgements—Appreciation is extended to the referee whose comments led to improvements of the paper. This work was supported in part by research grants from the Ministry of Science and Technology (MOST), Korea.

REFERENCES

1. J. Gerrard, The three-dimensional structure of the wake of a circular cylinder, *J. Fluid Mech.* **25,** 60–81 (1966).
2. W. Heine, On the investigation on vortex-excited pressure fluctuations, M.Sc. Thesis, University of British Columbia (1964).
3. P. Bearman, On vortex street wakes, *J. Fluid Mech.* **28,** 321–331 (1967).
4. A. K. M. F. Hussain and V. Ramjee, Periodic wake behind a circular cylinder at low Reynolds numbers, *Aero. Quartly* **123,** 123–142 (1976).
5. C. Barbi, D. P. Favier, C. A. Maresca and D. P. Telionis, Vortex shedding and lock-on of a cylinder in oscillatory flow, *J. Fluid Mech.* **170,** 527–544 (1986).
6. D. P. Telionis, M. Gundappa and T. E. Diller, On the organization of flow and heat transfer in the near wake of a circular cylinder in steady and pulsed flows, *ASME* **114,** 348–355 (1992).
7. G. J. Borell, B. K. Kim, W. Ekhaml, T. E. Diller and D. P. Telionis, Pressure and heat transfer measurement around a cylinder in pulsating crossflow. In *Unsteady Turbulence Boundary and Friction* (Edited by D. C. Wigger and C. S. Martin), pp. 17–23. ASME, New York (1985).
8. C. E. Andraka and T. E. Diller, Heat transfer distribution around a cylinder in pulsating crossflow, *ASME J. Engng Gas Turbines Power* **107,** 976–982 (1985).
9. M. Gundappa and T. E. Diller, The effects of freestream turbulence and flow pulsation on heat transfer from a cylinder in crossflow, *ASME J. Heat Transfer* **113,** 776–779 (1991).
10. J. Kestin and R. T. Wood, The influence of turbulence on mass transfer from cylinder, *ASME J. Heat Transfer* **93,** 321–327 (1971).
11. R. J. Goldstein and J. Karni, The effects of a wall boundary layer on local mass transfer from a cylinder in cross flow, *ASME J. Heat Transfer* **106,** 260–267 (1984).
12. H. J. Sung, M. S. Lyu and M. K. Chung, Experimental study on local convective mass transfer from a circular cylinder in uniform shear flow, *Int. J. Heat Mass Transfer* **34,** 59–68 (1991).
13. H. Miyazaki and E. M. Sparrow, Analysis of effects of freestream turbulence on heat transfer and skin friction, *ASME J. Heat Transfer* **99,** 614–619 (1977).
14. R. S. Seban, The influence of freestream turbulence on the local heat transfer from cylinders, *ASME J. Heat Transfer* **82,** 101–107 (1960).
15. B. Sunden, A theoretical investigation of the effects of freestream turbulence on skin friction and heat transfer for a bluff body, *Int. J. Heat Mass Transfer* **22,** 1125–1135 (1979).
16. H. H. Sogin and V. S. Subramanian, Local mass transfer from circular cylinders in cross flow, *ASME J. Heat Transfer* **83,** 483–493 (1961).
17. B. K. Kim, D. J. VandenBrink, M. S. Cramer and D. P. Telionis, Unsteady heat convection over circular cylinders, ASME Paper, No. 84-HT-100 (1984).
18. M. I. Boulos and D. C. T. Pei, Dynamics of heat transfer from cylinders in a turbulent air stream, *Int. J. Heat Mass Transfer* **17,** 767–783 (1974).